Received: 6 December 2021 | Revised: 11 January 2022 | Accepted: 5 February 2022

DOI: 10.1111/nan.12796

ORIGINAL ARTICLE

Neuropathology and Applied Neurobiology
JOURNAL OF THE BRITISH NEUROPATHOLOGICAL SOCIETY

WILEY

Absence of tissue transglutaminase reduces amyloid-beta pathology in APP23 mice

Micha M. M. Wilhelmus[1] | Osoul Chouchane[1] | Maarten Loos[2] | Cornelis A. M. Jongenelen[1] | John J. P. Brevé[1] | Allert Jonker[1] | John G. J. M. Bol[1] | August B. Smit[3] | Benjamin Drukarch[1]

[1]Department of Anatomy and Neurosciences, Amsterdam Neuroscience, Amsterdam UMC, Vrije Universiteit Amsterdam, Amsterdam, The Netherlands

[2]Sylics (Synaptologics BV), Amsterdam, The Netherlands

[3]Department of Molecular and Cellular Neurobiology, VU University Amsterdam, Amsterdam, The Netherlands

Correspondence
Micha M. M. Wilhelmus, Department of Anatomy and Neurosciences, Amsterdam UMC, De Boelelaan 1108, 1081 HZ Amsterdam, The Netherlands.
Email: m.wilhelmus@amsterdamumc.nl

Funding information
Proof-of-Concept Fund of Amsterdam Neuroscience, Grant/Award Number: PoC-2014-ND-06

Abstract

Aims: Alzheimer's disease (AD) is characterised by amyloid-beta (Aβ) aggregates in the brain. Targeting Aβ aggregates is a major approach for AD therapies, although attempts have had little to no success so far. A novel treatment option is to focus on blocking the actual formation of Aβ multimers. The enzyme tissue transglutaminase (TG2) is abundantly expressed in the human brain and plays a key role in post-translational modifications in Aβ resulting in covalently cross-linked, stable and neurotoxic Aβ oligomers.
In vivo absence of TG2 in the APP23 mouse model may provide evidence that TG2 plays a key role in development and/or progression of Aβ-related pathology.

Methods: Here, we compared the effects on Aβ pathology in the presence or absence of TG2 using 12-month-old wild type, APP23 and a crossbreed of the TG2−/− mouse model and APP23 mice (APP23/TG2−/−).

Results: Using immunohistochemistry, we found that the number of Aβ deposits was significantly reduced in the absence of TG2 compared with age-matched APP23 mice. To pinpoint possible TG2-associated mechanisms involved in this observation, we analysed soluble brain $A\beta_{1-40}$, $A\beta_{1-42}$ and/or $A\beta_{40/42}$ ratio, and mRNA levels of human APP and TG2 family members present in brain of the various mouse models. In addition, using immunohistochemistry, both beta-pleated sheet formation in Aβ deposits and the presence of reactive astrocytes associated with Aβ deposits were analysed.

Conclusions: We found that absence of TG2 reduces the formation of Aβ pathology in the APP23 mouse model, suggesting that TG2 may be a suitable therapeutic target for reducing Aβ deposition in AD.

KEYWORDS
Alzheimer's disease, amyloid-beta, APP23, transglutaminase

INTRODUCTION

Amyloid-beta (Aβ) protein deposition in the brain is a key pathological feature in Alzheimer's disease (AD). Two different types of aggregated Aβ protein brain deposits found in AD are senile plaques (SPs), that is, Aβ deposits in the brain parenchyma, and cerebral amyloid angiopathy (CAA), that is, Aβ deposits in the cerebral vessel walls [1]. Aβ protein is cleaved from its precursor Aβ precursor protein (APP) by secretases

into predominantly either $A\beta_{1-40}$ or $A\beta_{1-42}$ [2]. Aβ deposition as observed in AD brain is characterised by a shift from soluble monomers to toxic oligomers and eventually insoluble mature fibrils [3]. Although both $A\beta_{1-40}$ and $A\beta_{1-42}$ are known to self-aggregate, $A\beta_{1-42}$ is more prone to self-interact, resulting in proteolytically stable dimers, trimers and oligomers, so-called 'seeds', that drive the 'aggregated Aβ pathway' [4]. Since the discovery of the Aβ protein as the most abundant protein in SP and CAA, much progress has been made in unravelling the Aβ aggregation pathway both in vitro and in vivo. Unfortunately, the molecular mechanisms that result in the formation of stable Aβ 'seeds' that drive the aggregation pathway in vivo in AD are still largely unclear. Nonetheless, one of the mechanisms that is suggested to play a cardinal role in the formation of these 'seeds' is post-translational modifications of soluble Aβ species [5].

Tissue transglutaminase (TG), or transglutaminase 2 (TG2), is part of a protein family consisting of nine members. TGs are calcium-dependent enzymes that catalyse various reactions, including (gamma-glutamyl)polyamine bond formation, deamidation of protein substrates and the formation of stable intramolecular and intermolecular protein crosslinks [6]. This latter type of post-translational modification is the result of the fact that TGs are capable of forming covalent epsilon (gamma-glutamyl)lysine isopeptide bonds by catalysing an acyl transfer reaction between the gamma-carboxamide group of a polypeptide-bound glutamine and the epsilon-amino group of a polypeptide-bound lysine residue [6, 7]. TG2, the best characterised isotype of the TG family, is expressed throughout the human body and is abundantly present in the human brain [8]. Although believed to be catalytically dormant under physiological conditions [9], under pathological conditions, the enzyme changes its spatial conformation and switches into its catalytically active form [10]. As a result, TG2-catalysed isopeptide bonds may be formed that lead to the formation of stable and rigid protein–protein multimers and, ultimately, protein complexes [11, 12].

Evidence is mounting that TG2 is involved in the aggregation and accumulation of Aβ in AD [8, 9, 13, 14]. In AD brains, elevated levels of both TG2 and TG2-induced crosslinks have been found [15, 16], and in SP and CAA, TG2 protein and activity are observed [17–20]. Apart from the presence and activity of TG2 in SP and CAA of post-mortem AD cases, biochemical analysis demonstrated direct involvement of TG2 in the formation of Aβ-protein complexes and aggregates [12, 21, 22]. Both $A\beta_{1-40}$ and $A\beta_{1-42}$ are substrates of TG2-catalysed crosslinking, lower the oligomerisation threshold of Aβ self-aggregation, enhance Aβ-driven neurotoxicity in vitro and induce toxic protofibrils that inhibit long term potentiation in the CA1 regions of the hippocampus [12, 21–23]. However, despite the overwhelming histopathological and biochemical evidence, in vivo data on the role of TG2 in the development and/or progression of Aβ pathology is lacking.

To fill this gap in current knowledge and investigate the feasibility of considering TG2 as a potential future therapeutic target to counteract Aβ aggregation and deposition in the brain, we crossbred the Aβ-pathology-mimicking mouse model APP23, overexpressing human APP751 carrying the Swedish double mutation (K670M/N671L), with a TG2-knockout model [24, 25]. The APP23 mouse model is well characterised and demonstrates an age-dependent formation of both parenchymal Aβ deposition and Aβ deposition in the cerebral vessel wall [24]. The TG2 knockout model is generated by a genetic deletion of the TG2 gene and demonstrates no phenotypical differences when compared with wild-type (WT) mice [25]. In a previous study of our group, we performed an extensive distribution analysis of TG2 in the APP23 model and found association of both anti-TG2 antibody immunoreactivity and in situ TG2 activity with both parenchymal and cerebral vessel Aβ deposits in post-mortem brain tissue of APP23 mice, as well as in reactive astrocytes associated with these lesions [17]. Here, we investigated whether the absence of TG2 affects Aβ brain deposition in APP23 mice, that is, parenchymal Aβ and cerebral vessel Aβ. In addition, to better understand our observations, we analysed whether the lack of TG2 affects soluble $A\beta_{1-40}$ and $A\beta_{1-42}$ brain levels and ratio, mRNA levels of other TG family members, beta-pleated sheet formation in deposited Aβ and the presence of Aβ-lesion associated reactive astrocytes.

Key Points

- Ablation of TG2 reduced the formation of amyloid-beta deposits in APP23 mouse brain.
- Absence of TG2 had no effect on soluble brain amyloid-beta level and beta-pleated sheet formation.
- Absence of TG2 did not result in the increase of transglutaminase family members.
- Absence of TG2 did not affect glial formation associated with amyloid-beta pathology in APP23.
- TG2 plays a key role in the development and/or progression of amyloid-beta pathology.

MATERIALS AND METHODS

Animals

APP23 mice, overexpressing human APP751 carrying the Swedish double mutation (K670M/N671L) [24], were obtained from Novartis (a generous gift from Dr Derya R. Shimshek, Novartis Institutes of BioMedical Research, Neuroscience, Basel, Switzerland). TG2−/− mice were a generous gift from Prof. Gerry Melino, and generated by deletion of 1200 base pairs, from exon 5 to intron 6, which includes exon 6 containing the active site of TG2 [25], received on a mixed C57BL6/SVJ background. WT C57BL/6J mice were purchased from Charles River (L'Arbresie, France). In our facilities, APP23 and TG2 lines were maintained on a C57BL/6J background (Charles River) and group housed in standard mouse cages under conventional laboratory conditions with a 12:12-h light–dark cycle (light on at 8:00 AM, light

off at 8:00 PM), constant room temperature (22°C ± 2°C), humidity level (55% ± 5%) and food and water available ad libitum. Based on established milestones in the progression of AD pathology within the model (e.g., first appearance of plaques, cognitive deficits and progression of wide-spread Aβ pathology), 12-month-old animals were selected [26]. The 12-month-old mouse group consisted of APP23 ($n = 7$), WT ($n = 4$), APP23/TG2−/− ($n = 7$) and TG2−/− ($n = 2$).

Tissue collection

Animals were sacrificed at 12 months of age by cervical dislocation. The brains were harvested and dissected on ice into three parts: two hemi-forebrains and the cerebellum (the olfactory bulbs were discarded). After dissection, the brains were snap frozen in liquid nitrogen and immediately stored at −80°C until use.

Immunohistochemistry and double (immuno) fluorescence staining

Serial coronal sections of 6 μm were obtained, starting at the base of the hippocampus. The acquired sections were fixated for 10 min using 100% acetone, unless stated otherwise. Non-specific sites were blocked using bovine serum albumin (Capricorn Scientific, Ebsdorfergrund, Germany), except for the Aβ staining for which the sections were treated with milk powder. Endogenous peroxidases were quenched using a 0.3% H_20_2, 0.1% sodium azide solution in Tris-buffered saline (TBS, pH 7.6), for 15 min. All sections were incubated with their primary antibodies overnight at 4°C. All primary antibodies (Table S1) were diluted in a TBS-triton (0.5% Triton X) solution. Between the different incubation steps, sections were washed with TBS. The sections were stained for Aβ using a rabbit antihuman anti-amyloid antibody (715,800, dilution 1/400) purchased from Invitrogen (Carlsbad, CA, USA). For identification of astrocytes, the antiglial fibrillary acidic protein (GFAP) antibody (rabbit antibovine, dilution 1/400) obtained from DAKO (Santa Clara, CA, USA) was used. Guinea pig TG2 antigoat antibody (06471, dilution 1/4000) was obtained from Millipore (Temecula, CA, USA). To stain hyperphosphorylated tau, a mouse antihuman antibody recognising tau protein phosphorylated at both serine 202 and threonine 205 sites (AT8, dilution 1/2000) obtained from Innogenetics (Zwijnaarde, Belgium) was used. Sections stained for AT8 were fixated differently in different experiments, in 100% acetone and 4% PFA, respectively. All secondary antibodies were obtained from Jackson Immunoresearch (West Grove, PA, USA) all of which biotinylated and used in a 1/400 dilution: goat antirabbit, donkey antirat, donkey antigoat and goat antimouse antibodies. The complex of antibodies was recognised by the avidin–biotin–peroxidase complex, using the Vectastain Elite Avidin Biotin kit (Vector Laboratories, Burlingame, CA), for a period of 1 h. This was done in combination with 3,3′-diaminobenzidine (DAB) as chromogen (Sigma, St. Louis, MO). After the precipitation of DAB, sections were rinsed with Tris–HCL and subsequently washed with tap water before being dehydrated in a series of alcohol dilutions, after which the sections are covered in xylene and mounted with Entellan (Merck Millipore, Darmstadt, Germany). Counterstaining was performed using haematoxylin. After counterstaining, the sections were washed with tap water once more, before being dehydrated in a series of alcohol dilutions, after which the sections were covered in xylene and mounted with Entellan (Merck Millipore). Besides brightfield imaging techniques, multiple fluorescent stains were executed using fluorescent dyes and antibodies. To check for the presence of β-pleated sheets in dense core amyloid plaques, double staining was performed utilising thioflavin S and the aforementioned anti-Aβ primary antibody in combination with a biotinylated, goat antirabbit, secondary antibody coupled to Alexa594 (1:400, Molecular Probes, Amsterdam, The Netherlands).

Quantification of immunohistochemical staining

Using a Leica brightfield microscope (DM5000B, Leica Microsystems, Wetzlar, Germany) equipped with a nuance spectral imager (Nuance 3.02, Perkin Elmer Inc., Hopkinton, MA), two serial Aβ stains were photographed per cohort, with an average of 30 μm (a minimum of 18 μm) spacing between sections of the same animal. The quantification of the Aβ burden was accomplished by performing a surface measurement of Aβ carried out by capturing a section in four photos at a magnification of 2.5×, following the protocol by Hepp et al. [27]. The load of Aβ pathology was represented by the percentage of the section that is covered by Aβ. In order to determine what fraction of the surface area in a section is overlaid with Aβ pathology, the multispectral imaging system used the individual spectra of DAB and haematoxylin. After discriminating between the spectra of DAB and haematoxylin, the nuance software, using the colocalisation tool, was able to compute the fraction of Aβ represented by DAB that colocalises with the haematoxylin background. To distinguish which threshold should be implemented, a test was performed with multiple sections containing a wide variety of Aβ pathology. The threshold was set at 0.200 for haematoxylin and 0.938 for Aβ, respectively. After calculating the percentage of Aβ pathology, the values of two slides per mouse were averaged, representing the Aβ burden per mouse. Except for the quantification of Aβ pathology, a morphological quantification was performed to evaluate the differences between APP23 and APP23/TG2−/− mice in the amount of individual amyloid manifestations. To do so, the protein deposits were divided into three morphology-based categories: SPs, small dense plaques and vascular amyloid deposits, respectively (see Figure 1A). SPs are defined as parenchymal Aβ deposits of ∼20–60 μm in diameter, whereas small dense plaques are ∼2–10 μm in diameter. Vascular amyloid deposits are defined as Aβ deposits in the brain vasculature. The morphological quantification was performed by manually appointing the individual forms of Aβ deposits to one of the categories and counting these at a magnification of 4× using an Olympus Brightfield microscope (Vanox-T., Olympus Life Science Solutions, Shinjuku, Tokyo, Japan). The Aβ depositions in the hippocampus were counted separately from the

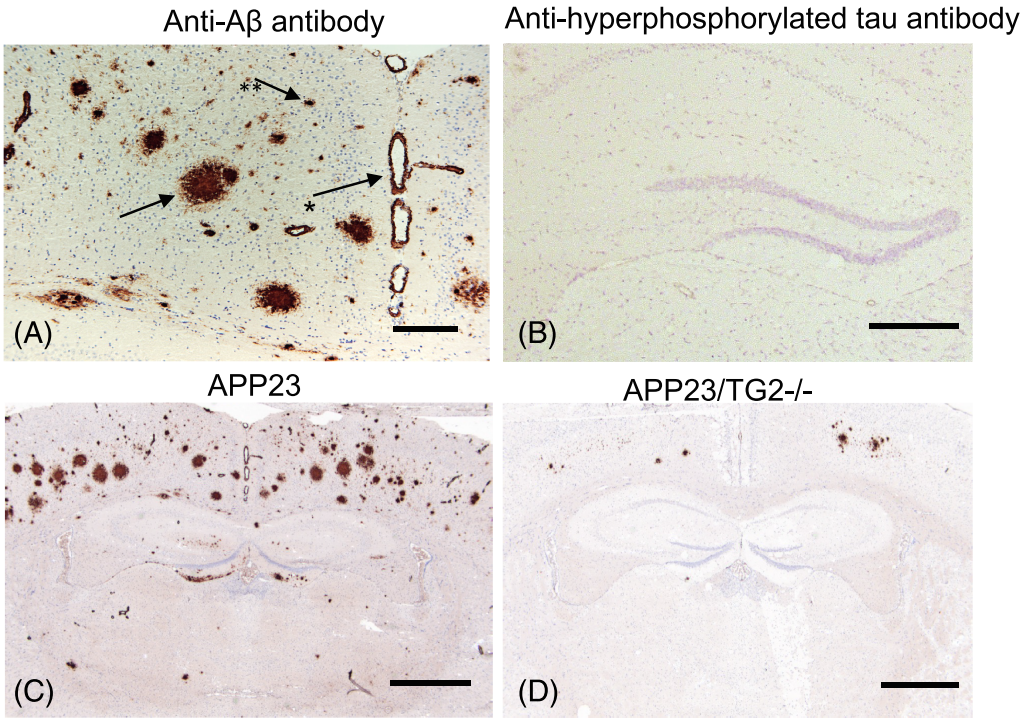

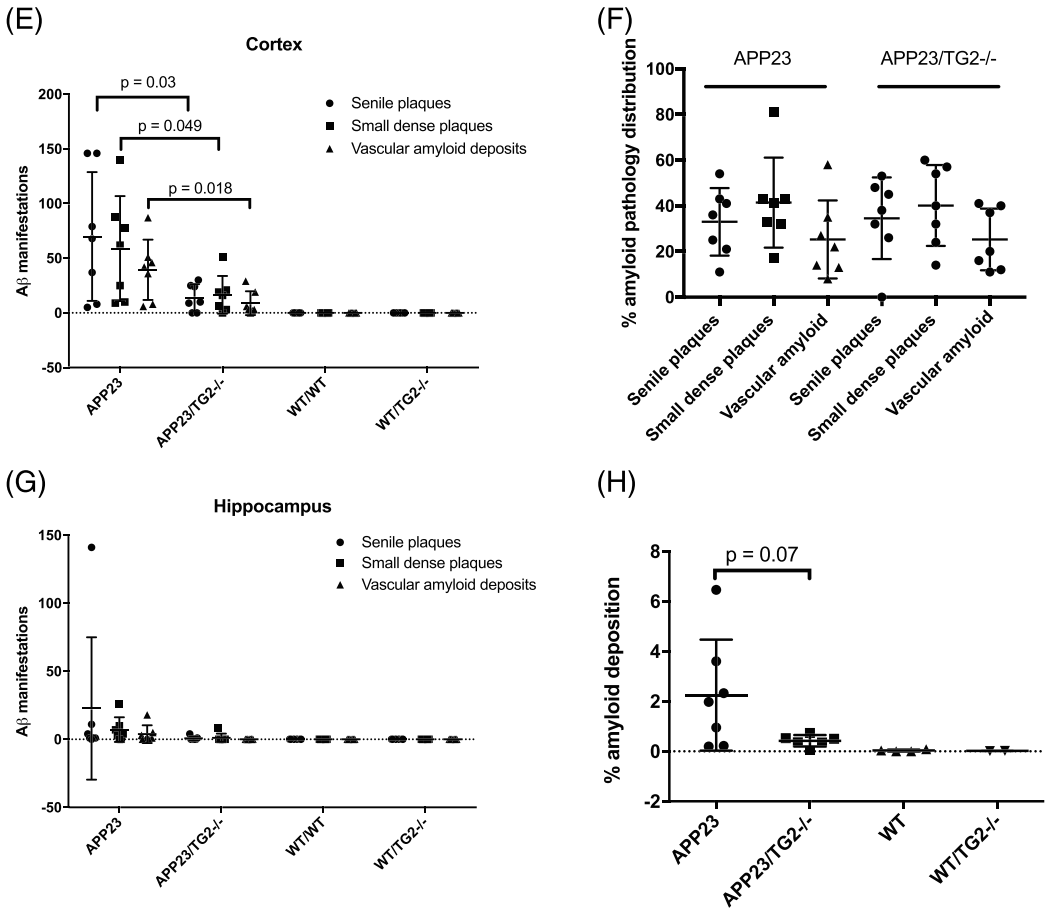

FIGURE 1 Legend on next page.

FIGURE 1 Distribution of Aβ and hyperphosphorylated tau in APP23/TG2−/− and APP23 mice brain and quantification of Aβ pathology in APP23/TG−/− and APP23 mice. (A) Analysis of Aβ deposits in post-mortem cryo-fixed brain tissue of 12-month-old mice APP23 mice demonstrated different types of Aβ deposits in the cortex, that is, senile plaques (arrow), vascular amyloid deposits (arrow, asterisk) and small dense plaques (arrow, double asterisk). (B) In APP23 mice, antihyperphosphorylated tau antibody immunoreactivity (AT8) was absent. (C) Analysis of APP23 mice using the anti-Aβ antibody immunoreactivity demonstrated antibody immunoreactivity of Aβ deposits. (D) In age-matched APP23/TG2−/− mice, a reduction in the number of Aβ deposits was observed when compared with APP23 mice. The number of Aβ lesions was quantified in both hippocampus and cortex of 12-month-old mice. (E–H) No anti-Aβ antibody immunoreactive deposits were found in both the hippocampal and cortex region of WT and WT/TG2−/− mice. (E) In the cortex region of APP23/TG2−/− mice, a significant reduction in the number of senile plaques ($p = 0.03$), small dense core plaques ($p = 0.049$) and vascular deposits ($p = 0.018$) was found, when compared with APP23 mice. (F) The percentage of various types Aβ deposits, that is, senile plaques, small dense core plaques and vascular amyloid, were determined with respect to the total deposits analysed. (G) In the hippocampus of APP23 and APP23/TG2−/− mice, no significant differences in Aβ deposits were observed between groups. The percentage of anti-Aβ antibody immunoreactivity was analysed as a percentage of total surface area of the brain slide. (H) The percentage of total brain anti-Aβ antibody immunoreactivity in APP23/TG2−/− mice was reduced, albeit not statistically significant, when compared with age-matched APP23 mice ($p = 0.07$). Scale bars: (A,B) 60 μm, (B,C) 1000 μm. Abbreviations: WT, wild type; TG2, transglutaminase 2; Aβ, amyloid-beta

depositions in the rest of the brain. Fraction of the surface area in a section positive for anti-GFAP antibody immunoreactivity was quantified similar as to the above-described Aβ. Of each animal, two cortical regions in separate sections were manually selected to quantify the percentage of anti-GFAP immunoreactivity as a percentage of total brain surface area (Figure 5G). The percentage of anti-GFAP immunoreactivity of both regions was averaged for each animal.

Semiquantitative RT-PCR

To determine mRNA transcript levels in all mice, brain tissue was homogenised in Trizol reagent (Invitrogen, Carlsbad, CA, USA). Total RNA was isolated, and 1 μg cDNA was synthesised using the Reverse Transcription System (Promega, Madison, WI, USA) with oligo-dT primers and AMV enzyme according to the manufacturer's instructions. For semiquantitative RT-PCR, the SYBR Green PCR Core reagents kit (Applied Biosystems, Foster City, CA, USA) was used. Amplification of cDNA was performed in MicroAmp Optical 96-well Reaction Plates (Applied Biosystems) on an ABI PRISM 7700 Sequence Detection System (Applied Biosystems). The reaction mixture (20 μl) was composed of 1× SYBR Green buffer, 3 mM $MgCl_2$, 875 μM dNTP mix with dUTP, 0.3 U AmpliTaq gold, 0.12 U Amperase UNG, 12.5 ng cDNA and 15 pmol of each primer (Table S1). The reaction conditions were an initial 2 min at 50°C, followed by 10 min at 95°C and 40 cycles of 15 s at 95°C and 1 min at 59°C. The mRNA expression levels were quantified relative to the level of the housekeeping gene glyceraldehyde-3-phosphate-dehydrogenase (GAPDH) using the following calculation: $2^{-(\text{Threshold cycle of target mRNA "–" Threshold cycle of GAPDH})} \times 100$.

Western blotting

After gel electrophoresis, samples were transferred to a 0.2 μm nitrocellulose membrane (Li-COR Biosciences, Lincoln, NE, USA) and blocked with Odyssey blocking buffer (Li-COR Biosciences) diluted 1:1 in TBS (Li-COR-TBS) for 1 h at room temperature. Blots were incubated overnight at 4°C with primary antibody, that is, mouse anti-Aβ (clone 82E1, IBL International, Deventer, The Netherlands, dilution 1:1000) in Li-COR-TBS with 0.1% Tween-20 (Sigma-Aldrich). Subsequently, blots were incubated with secondary antibodies donkey antimouse coupled to IRDye 680 (dilution 1:10,000, Li-COR Biosciences). In between incubation steps, blots were extensively washed with TBS with 0.1% Tween-20 and TBS alone. Blots were visualised with the Odyssey Sa infrared imaging system (Li-COR Biosciences).

$A\beta_{1-40}$ and $A\beta_{1-42}$ protein analysis

The concentration of $A\beta_{1-x}$, $A\beta_{1-40}$ and $A\beta_{1-42}$ in the soluble protein fraction was determined by ELISA measurements using the human $A\beta_{1-x}$ assay kit, the human $A\beta_{1-40}$ assay kit and the human $A\beta_{1-42}$ assay kit (IBL International). All samples were diluted to within the detection limits of the test and analysed in duplicate according to the manufacturer's instructions. The $A\beta_{1-x}$ assay detects all Aβ variants with an intact N-terminus and a length of more than 16 amino acids. The $A\beta_{1-40}$ assay shows ≤0.1% cross-reactivity with other human Aβ species but does show 16.3% cross-reactivity with endogenous $A\beta_{1-40}$. The $A\beta_{1-42}$ assay shows ≤0.1% cross-reactivity with other human Aβ species and endogenous Aβ (manufacturer's instructions).

Statistical analysis

Non-parametrical statistical analyses with exact significance values were used for all group comparisons. Comparisons between the genotype groups were performed using the independent-sample Mann–Whitney *U* test. Differences between the various age groups were evaluated with the independent-sample Kruskal–Wallis test. Post hoc analysis between specific age groups was performed using the independent-sample Mann–Whitney *U* test with a Bonferroni correction for multiple comparisons. Outliers with a high coefficient of variation (≥20%) between duplicate measurements were excluded from statistical analysis. All statistical tests were performed using SPSS

statistics software v22.0 (IBM). All graphs were created using Graphpad Prism v5.03 (Graphpad, San Diego, CA, USA).

RESULTS

Absence of both TG2 mRNA and protein in APP23/TG−/− mice

To confirm the complete absence of both TG2 mRNA (TGM2) and protein in the newly developed crossbred APP23/TG2−/− mice, TGM2 mRNA and TG2 protein expression were analysed in brain homogenates of APP23, WT, APP23/TG2−/− and TG2−/− mice. In both APP23 ($n = 6$) and WT ($n = 4$) mice, TGM2 mRNA was observed (Figure S1A). Interestingly, we found a trend in the average TGM2 mRNA levels showing higher levels in the APP23 mice compared with WT mice, albeit not significant due to the large variation in TGM2 levels within groups (Figure S1A). In contrast, in both WT/TG2−/− ($n = 2$) and APP23/TG2−/− ($n = 7$) mice, TGM2 mRNA levels were below the detection limit (Figure S1A). Similarly, Western blot analysis of TG2 protein expression demonstrated the presence of TG2 protein (~78 kDa) in APP23 mice ($n = 4$, Figure 1B) and WT mice ($n = 4$, not shown), whereas no TG2 protein was detectable in both APP23/TG2−/− mice ($n = 4$, Figure 1B) and TG2−/− mice ($n = 2$, data not shown).

Distribution of Aβ pathology in APP23 and APP23/TG2−/− mice brain

In APP23 mice, initial Aβ deposits are observed at the age of 6 months and increase thereafter in both number and surface area with age [24]. In cryo-fixed post-mortem brain tissue of 12-month-old APP23 mice, different types of Aβ deposits were observed, that is, vascular amyloid deposits and parenchymal Aβ deposits, divided into SPs and small dense plaques (Figure 1A). Although hyperphosphorylated tau pathology has been described in 12-month-old mice APP23 mice [28], no anti-hyperphosphorylated tau immunoreactivity was observed (Figure 1B). To analyse the effect of the deletion of TG2 on Aβ deposits, immunohistochemical analysis using an antihuman Aβ antibody was performed on all animals. Anti-Aβ antibody immunoreactivity demonstrated the presence of Aβ deposits in APP23 mice (Figure 1C). In APP23/TG2−/− mice, a strong reduction in the total number of Aβ deposits was observed when compared with the APP23 mice (Figure 1D).

Reduced Aβ pathology in APP23/TG−/− mice compared with APP23 mice

As described above, a reduction of anti-Aβ antibody immunoreactivity in APP23/TG2−/− mice was found when compared with age-matched APP23 mice. In order to quantify the effect of the absence of TG2 on the different types of Aβ lesions observed in these mice, differences in number of Aβ lesions were quantified in both hippocampus and cortex. We found no anti-Aβ antibody immunoreactive deposits in the hippocampal and cortex region of WT and WT/TG2−/− mice (Figure 1E,G). In the cortex region of 12-month-old APP23/TG2−/− mice, a significant reduction in the number of SPs ($p = 0.03$), small dense plaques ($p = 0.049$) and vascular deposits ($p = 0.018$) was found, when compared with APP23 mice (Figure 1E). To investigate whether the absence of TG2 also affected the type of Aβ deposits formed, we analysed the percentage of SPs, small dense plaques and vascular amyloid compared with the total lesion count. However, no significant differences were found between APP23 and APP23/TG2−/− mice in the percentage of SPs, small dense plaques or vascular amyloid deposits with respect to the total count of Aβ deposits (Figure 1F). In other words, no shift in the pattern of Aβ pathology occurred as a consequence of TG2 deletion. In the hippocampal region, Aβ deposition was limited and only present in a subset of mice (Figure 1G); therefore, no statistical comparison between the number of Aβ deposits found between the different mice groups was performed. To determine whether the absence of TG2 significantly affects the overall Aβ load in these mice, the percentage of anti-Aβ antibody immunoreactivity was analysed as a percentage of total brain surface area [27] (see Section 2). As expected, in both WT and WT/TG2/−/− mice, no Aβ deposits were detected (Figure 1H). However, in line with our immunohistochemical observations and quantitative analysis of the individual Aβ lesions, the percentage of total brain anti-Aβ antibody immunoreactivity in APP23/TG2−/− mice was strongly reduced when compared with APP23 mice, albeit not statistically significant (Figure 1H).

Effects of the absence of TG2 on soluble brain $Aβ_{1-40}$ and $Aβ_{1-42}$ levels, or $Aβ_{40/42}$ ratio in APP23 and APP23/TG2−/− mice

Aβ is a known substrate of TG2 crosslinking activity, resulting in the formation of stable Aβ multimers [12, 21, 22]. Absence of TG2 might therefore affect the formation of such multimers and, as a consequence, the level of soluble Aβ monomers. For this reason, we determined whether deletion of TG2 affected the levels of soluble brain $Aβ_{1-40}$, $Aβ_{1-42}$ and/or the $Aβ_{40/42}$ ratio using a dedicated ELISA to analyse soluble human $Aβ_{1-40}$ and $Aβ_{1-42}$ in mouse brain homogenates. Although a trend towards reduction in both soluble brain $Aβ_{1-40}$ and $Aβ_{1-42}$ levels was observed in APP23/TG2−/− mice compared with APP23 mice, this difference failed to reach statistical significance (Figure 2A,B). Also, analysis of $Aβ_{1-40}/Aβ_{1-42}$ ratio demonstrated no significant difference in soluble $Aβ_{1-40}/Aβ_{1-42}$ ratio between APP23 and APP23/TG2−/− mice (Figure 2C).

Analysis of mRNA of human APP, mouse TGM1, TGM2, TGM3, TGM6 and FXIIIA in mouse brain homogenates

In order to gain more insight into the underlying mechanisms that result in reduced Aβ pathology in APP23/TG−/− mice compared with

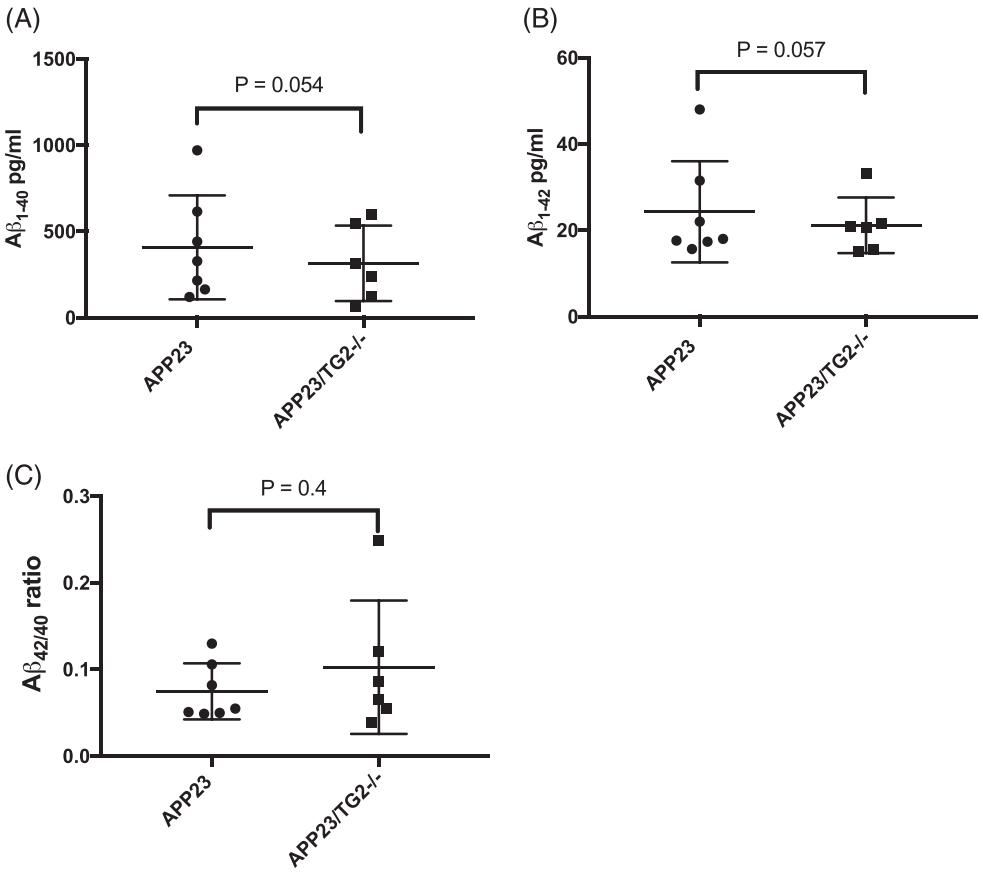

FIGURE 2 Analysis of soluble brain $A\beta_{1-40}$ and $A\beta_{1-42}$ levels and $A\beta_{40/42}$ ratio in APP23 and APP23/TG2−/− mice. Soluble human $A\beta_{1-40}$, $A\beta_{1-42}$ and $A\beta_{1-40}/A\beta_{1-42}$ ratio were analysed in mouse brain homogenates. (A,B) Reduction in both soluble brain $A\beta_{1-40}$ and $A\beta_{1-42}$ levels were found in APP23/TG2−/− mice compared with APP23 mice, albeit not significant. (C) No significant difference in soluble brain $A\beta_{1-40}/A\beta_{1-42}$ ratio was found between APP23 and APP23/TG2−/− mice. Abbreviations: TG2, transglutaminase 2; Aβ, amyloid-beta

APP23, mRNA levels of both APP and of TG2 family members, known to be expressed in both human and mouse brain, that is, TG1 (TGM1), TG3 (TGM3), TG6 (TGM6) and FXIIIa, were analysed. Analysis of the mRNA levels in mouse brain homogenates demonstrated no significant difference in human APP mRNA levels between APP23 and APP23/TG2−/− (Figure 3A). Human APP mRNA was not detectable in both WT and WT/TG2−/− mice (Figure 3A). Analysis of TG2 family members present in the mouse brain demonstrated no significant increase in mRNA levels between APP23 or WT and their TG2−/− counterparts for either TGM1 (Figure 3B), TGM3 (Figure 3C), FXIIIA (Figure 3D) or TGM6 (data not shown as TGM6 mRNA level were not significantly higher compared with background).

Effects of the absence of TG2 on beta-pleated-sheet Aβ deposition

Aβ accumulation and deposition in AD brain lesions, that is, SP and CAA, is characterised by beta-pleated sheet formation [29]. This typical 3D structure of deposited Aβ is histologically recognised by thioflavin S staining [30]. Crosslinking of TG2 substrates, such as Aβ, by TG2's transamidation reaction results in covalent protein complexes [12, 22, 31]. However, it is known that upon TG2-catalysed crosslinking of other self-aggregating, neurodegenerative disease-associated, proteins alternative protein complexes are formed [11]. In fact, TG2-catalysed crosslinking of self-aggregating neurodegenerative proteins may lead to 'off-pathway' protein complexes lacking a beta-pleated sheet. This has been shown previously by us for alpha-synuclein [11]. In order to investigate whether the deletion of TG2 in APP23/TG2−/− mice affects the 3D structure of Aβ deposits, that is, the presence of beta-pleated sheets in SP and CAA, double staining of an anti-Aβ antibody and thioflavin S staining was performed on cryo-fixed post-mortem APP23 and APP23/TG2−/− brain tissue. In both APP23 (Figure 4A–C) and APP23/TG2−/− (Figure 4D–F) mice, double staining was found of anti-Aβ antibody immunoreactivity and thioflavin S staining in the majority of SPs (Figure 4A) and CAA (not shown), suggesting that the presence or absence of TG2 does not visibly affect beta-pleated sheet formation in Aβ deposits.

Effects of the absence of TG2 on the presence of reactive astrocytes associated with Aβ deposition

TG2 is expressed in reactive astrocytes associated with both human and mice Aβ deposits [17, 18]. In APP23 mice, TG2 is present in anti-GFAP antibody immunoreactive astrocytes, whereas no colocalisation of anti-TG2 staining with microglial cells associated with Aβ deposits was observed [17]. We therefore investigated whether the presence of reactive astrocytes, associated with Aβ pathology, was affected by

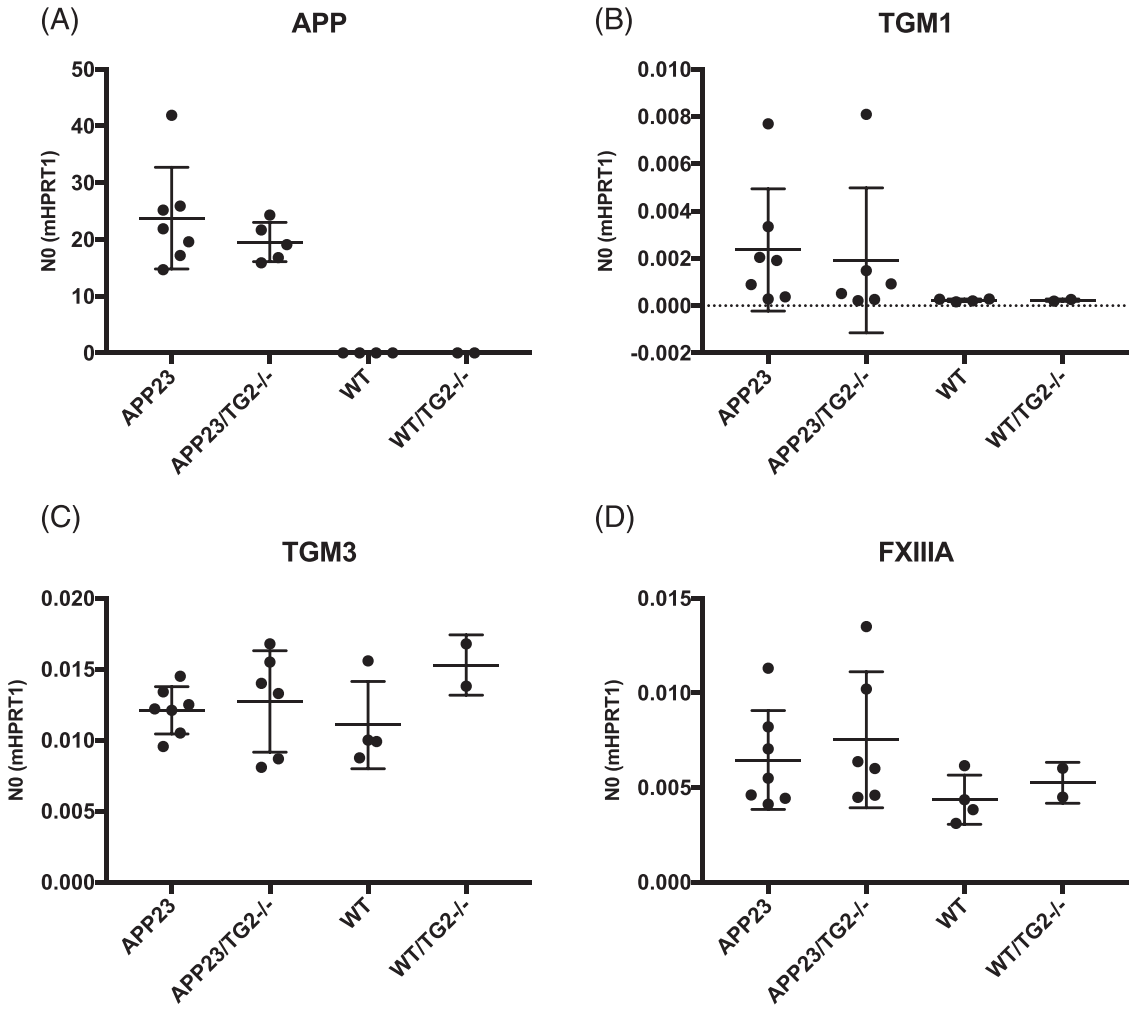

FIGURE 3 Analysis of mRNA of human APP, mouse TGM1, TGM3, TGM6 and FXIIIA in mouse brain homogenates. Levels of mRNA of APP, TGM1, TGM3, TGM6 and FXIIIA were analysed in mouse brain homogenates of WT, TG2−/−, APP23, APP23/TG2−/− and APP23/TG2+/−. (A) No significant difference in human APP mRNA levels were found between APP23 and APP23/TG2−/− mice. No significant difference in mRNA levels between all groups was found for (B) TGM1, (C) TGM3 and (D) FXIIIA. Abbreviations: TG2, transglutaminase 2; TGM1, transglutaminase 1 coding gene; TGM3, transglutaminase 3 coding gene; APP, amyloid-beta precursor protein coding gene; FXIIIa, factor 13a

deletion of TG2. For this purpose, immunohistochemical analysis was performed on murine post-mortem tissue, using an anti-GFAP antibody. In both APP23 and APP23/TG2−/− mice, association of GFAP-positive astrocytes with Aβ deposits was observed (Figure 5A–H). In order to quantify the presence of GFAP-positive astrocytes in association with Aβ deposits, two cortical brain areas were selected in each animal (APP23, APP23/TG2−/−, WT and WT/TG2−/−) to determine the percentage of GFAP-positive surface area (Figure 5G). The average of the percentage of GFAP-positivity of both selected areas for each animal was determined and plotted as the percentage of positive GFAP area (Figure 5H). In both APP23 and APP23/TG2−/− mice, an increase in GFAP-positive surface area in the cortical region was found compared with WT and WT/TG2−/− mice, respectively. However, no differences in GFAP-positive surface area were observed between APP23 and APP23/TG2−/− mice ($p = 0.95$) (Figure 5H). In APP23 mice, a sex-related difference in the number of reactive astrocytes associated with Aβ lesions has been suggested as female APP23 mice demonstrated higher numbers of reactive astrocytes associated with Aβ lesions when compared with male APP23 mice [32]. However, we did not find statistically significant gender-related differences in the percentage of anti-GFAP antibody immunoreactivity between male and female APP23 mice ($p = 0.64$) or APP23/TG2−/− mice ($p = 0.53$) (Figure S2). We also did not observe statistically significant gender-related effects in the percentage of anti-GFAP antibody immunoreactivity between male APP23 and APP23/TG2−/− mice ($p = 0.57$) or between female APP23 and APP23/TG2−/− mice, respectively ($p = 1.0$) (Figure S2). In line with earlier findings [17], microglial staining of both APP23 and APP23/TG2−/− mice, using the AD-associated microglial markers anti-CD45 and CD68 antibodies [33], demonstrated the presence of microglial cells in a small subset of Aβ deposits which, however, did not differ between APP23 and APP23/TG2−/− mice (Figure S3).

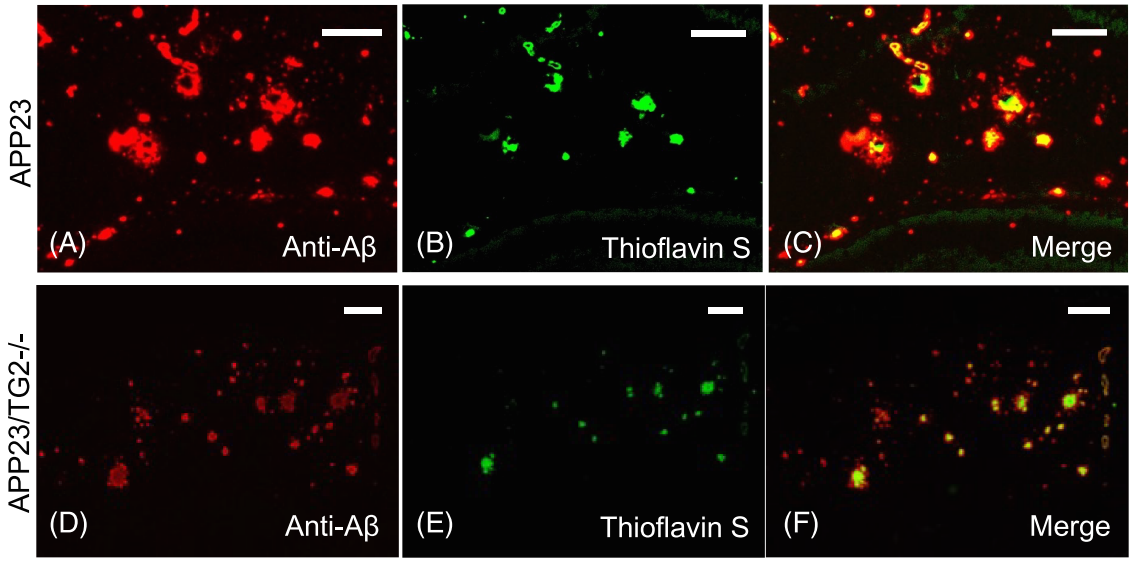

FIGURE 4 Analysis of beta-pleated-sheet Aβ deposition in APP23 and APP23/TG2−/− brain tissue. Double immunofluorescence staining of an anti-Aβ antibody and thioflavin S was performed on cryo-fixed post-mortem APP23 and APP23/TG2−/− brain tissue of 12-month-old animals. Analysis of distribution of Aβ deposits positive for both the anti-Aβ antibody and thioflavin S staining in brain tissue of (A–C) APP23 and (D–F) APP23/TG2−/− mice showed no apparent difference. Scale bars: (A–F) 60 μm. Abbreviations: TG2, transglutaminase 2; Aβ, amyloid-beta

DISCUSSION

Here, we set out to investigate in vivo effects of the absence of TG2 on the development of Aβ pathology in a well-characterised AD animal model. Analysis of Aβ deposits demonstrated a significant reduction in Aβ pathology, that is, the number of vascular amyloid deposits and parenchymal Aβ deposits, in 12-month-old APP23/TG2−/− mice as compared with APP23 mice. In an attempt to better understand TG2-associated mechanisms linked to this reduced Aβ pathology in APP23/TG2−/− mice, we also analysed levels of soluble brain $A\beta_{1-40}$, $A\beta_{1-42}$ and $A\beta_{40/42}$ ratio and brain expression of human APP, mouse TGM1, TGM2, TGM3, TGM6 and FXIIIA mRNA in the various mouse models. In addition, we addressed both beta-pleated sheet formation in Aβ deposits and the presence of reactive astrocytes and microglial cells associated with the Aβ deposits. However, besides the clear and statistically significant reduction in the number of amyloid deposits, none of the above-mentioned parameters were found to be significantly different between APP23 and APP23/TG2−/− animals.

Until now, in vivo evidence on the role of TG2 in protein aggregation in neurodegeneration was limited to Parkinson's and Huntington's disease mouse models (review by Wilhelmus et al. [9]). Although somewhat controversial, in Huntington's disease mouse models, the absence of TG2 results in an increase in soluble aggregated Huntingtin protein [34, 35], whereas in synuclein overexpression-based mouse models of Parkinson's disease, the absence of TG2 results in reduced phosphorylated alpha-synuclein aggregates [36]. In contrast, despite the accumulating evidence of TG2's role in the development and progression of Aβ pathology [9], that is, histopathological and biochemical data, in vivo evidence on the role of TG2 in Aβ aggregation and deposition was lacking thus far. We here demonstrate for the first time that the absence of TG2 reduced three major forms of Aβ deposits observed immunohistologically in the APP23 mouse model [24]. In the cortex, we observed that the number of SPs, small dense plaques and vascular Aβ deposits were significantly higher in APP23 mice when compared with APP23/TG2−/− mice. These findings demonstrate that the absence of TG2 reduces and/or delays the formation of all types of observed Aβ lesions in APP23 mice, confirming previous publications hinting towards a cardinal role for TG2 in Aβ aggregation and deposition [9, 13]. In contrast to the cortex, however, hippocampal Aβ lesions were only found in small numbers, in both APP23 and APP23/TG2−/− mice, albeit APP23 mice demonstrated overall higher numbers of hippocampal Aβ lesions compared with APP23/TG2−/−. Our observation that smaller numbers of Aβ lesions are observed in the hippocampus compared with the cortex regions in 12-month-old APP23 is in line with previous observations [37], and although we did find a significant quantitative difference between the individual types of Aβ lesions between APP23 and APP23/TG2−/− mice, respectively, a large variation in the total number of pathological Aβ lesions (ranging from >10 Aβ lesions up to 150 in the same selected brain area) were observed in the APP23 mouse group. This may (partly) explain why *overall* Aβ deposit load was not significantly different between both mouse groups. Moreover, the anti-Aβ antibody immunoreactive surface area in the APP23 mouse group, ranged from almost absence of Aβ deposits to covering ∼6.5% of total brain area. This serves to illustrate that 12-month-old APP23, despite the apparent similar genetic background, housing and reported onset of Aβ pathology at the age of 6 months [24], display a high variety in Aβ deposit load. As we used both male and female APP23 mice, sex differences might play a role in differences in Aβ load at this age [32]. However, both male and female mice were

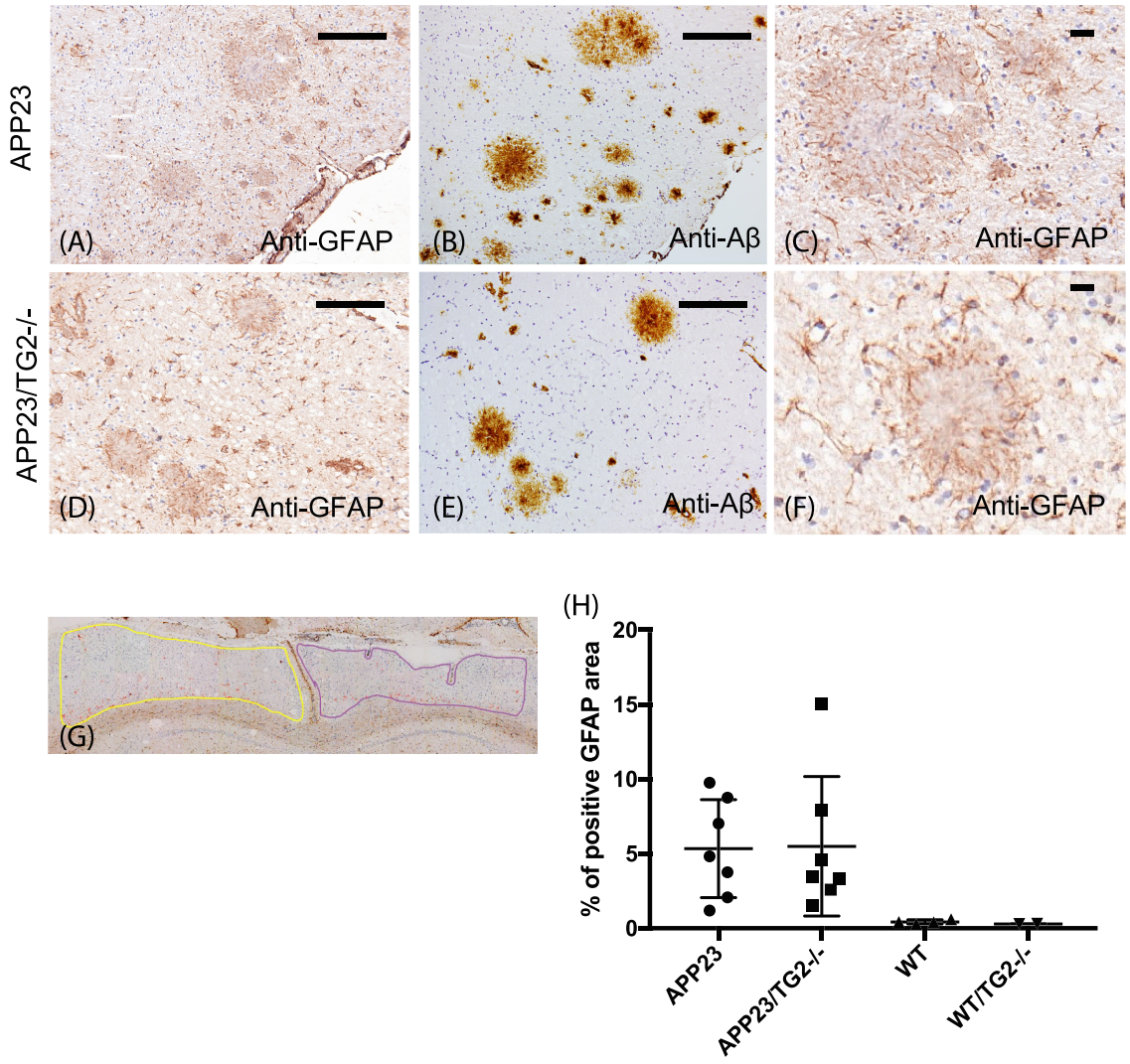

FIGURE 5 Analysis of deposited Aβ-associated glial activity in APP23 and APP23/TG2−/− brain tissue. Analysis of the distribution pattern of reactive astrocytes, associated with Aβ pathology in both 12-month-old APP23 and APP23/TG2−/− mice, was performed using immunohistochemistry with an anti-GFAP antibody. In Aβ deposits of both APP23 and APP23/TG2−/− mice, activated astrocytes (A–F) were observed. The percentage of GFAP staining of the total tissue area of two cortical regions (G, example) was analysed for each animal (APP23, APP23/TG2−/−, WT and WT/TG2−/−) and averaged per animal (H). Scale bars: (A–F) 60 μm. Abbreviations: TG2, transglutaminase 2; Aβ, amyloid-beta; GFAP, glial fibrillary acidic protein; WT, wild type

equally distributed among groups demonstrating either a high or low Aβ load, suggesting that sex did not contribute to the observed large range in Aβ load within the APP23 group. Finally, it has been demonstrated that hyperphosphorylated tau inclusions representing neuronal pathology, using the well-characterised and often used AT8 antibody, are present in 12-month-old APP23 mice [24]. However, despite our long-standing experience using the AT8 antibody on both cryo-fixed mouse and human brain sections [18, 38–41], we did not find any immunohistochemical staining using this antibody in our tissue sections of both APP23 and APP23/TG2−/− mice.

In order to obtain more information on possible mechanisms linking the lack of TG2 protein to the observed reduction in Aβ pathology in APP23 mice, we analysed soluble $A\beta_{1-40}$ and $A\beta_{1-42}$ levels and determined the $A\beta_{40/42}$ ratio. The measured soluble $A\beta_{1-40}$ and $A\beta_{1-42}$ levels in our study are in line with previous reports on 12-month-old APP23 mice, in which an ~10-fold increase in soluble $A\beta_{1-40}$ compared with $A\beta_{1-42}$ is reported [42]. Although we did find reduced levels of both soluble $A\beta_{1-40}$ and $A\beta_{1-42}$ in APP23/TG2−/− mice compared with APP23, due to the large variation within groups, no statistical significance was reached at group level. An interesting observation in light of TG2's role in Aβ deposition was the lack of differences found in beta-pleated sheet formation of Aβ lesions between APP23 and APP23/TG2−/− mice. As stated above, TG2-catalysed crosslinking of self-aggregating neurodegenerative proteins may lead to alternative, 'off-pathway', protein complexes lacking a beta-pleated sheet. This has been shown previously by us for alpha-synuclein [11]. According to this

idea, absence of TG2 might result in higher levels of beta-pleated sheet-positive Aβ deposition and thus an increase in Aβ deposition. However, the lack in differences found in Aβ deposits positive for beta-pleated sheets between APP23 and APP23/TG2−/− suggests that despite the absence of TG2, beta-pleated sheet formation in Aβ deposits remains unaffected.

The absence of TG2 in APP23/TG2−/− animals might lead to an increase in expression of other TGs as an attempt to compensate for the loss of TG2's function in vivo. TG2 family members found in the brain, for example, TG1, TG3, TG6 and FXIIIa, might therefore take over the TG2 (crosslinking) activity in the APP23/TG2−/− mouse brain. As in a Parkinson's disease model using TG2−/− animals, it was demonstrated that other TG2 isoform take over TG2's crosslinking activity in mitochondria [43]. In addition, recent discoveries of our group demonstrated that in neurofibrillary tangles in AD, besides TG2, TG1 is also present and might also be involved in the crosslinking of hyperphoshorylated tau, whereas FXIIIa might be involved in the crosslinking of Aβ in CAA [41, 44]. Furthermore, our current observation of increased TGM1 expression under pathological conditions, that is, APP23 and APP23/TG2−/− mice, is in line with previous findings of our group demonstrating upregulated TG1 expression in an AD model mimicking neurotoxicity [38]. However, no upregulation in mRNA levels of TG1, TG3, TG6 or FXIIIa was found between APP23 and APP23/TG2−/− mice, although it remains to be elucidated whether other TG isoforms replace TG2 crosslinking or other functions at the protein level in APP23/TG2−/− mice.

In AD, reactive astrocytes immunopositive for anti-TG2 antibodies are associated with SPs and CAA [18, 19]. In line with these observations, in AD mouse models, such as the APP/PS1 [45] and APP23 model, anti-TG2 antibody immunoreactivity is found in astrocytes associated with both parenchymal and vascular Aβ deposits [17]. Although the exact function of this TG2 in reactive astrocytes associated with AD brain lesions in humans and animal models remains to be elucidated, it has been suggested that TG2, produced and released by astrocytes, plays a role in adhesion and migration of astrocytes by modifying the local extracellular matrix via crosslinking of extracellular matrix proteins [19, 46–48]. Although our observations in the current study of anti-GFAP antibody immunoreactivity in astrocytes associated with Aβ deposits in APP23 mice are in line with our previous findings [17], we did not observe statistically significant differences in the percentage of anti-GFAP antibody immunoreactivity in regions with Aβ deposits between APP23 and APP23/TG2−/− mice. However, possible effects may have been obscured by the large spread (i.e., variation) in percentage of anti-GFAP antibody immunoreactivity within each mouse group. Despite this uncertainty, these data do suggest that lack of (astrocytic) TG2 does not affect the presence of GFAP-positive astrocytes surrounding (the reduced number of) parenchymal amyloid deposits in APP23 mice. We did observe a significant increase in GFAP-positive astrocytes in similar brain areas between APP23 and WT or TG2−/− animals, and between APP23/TG2−/− and WT or TG2−/− animals, suggesting that overexpression and/or deposition of human Aβ in mouse brains induce GFAP expression in astrocytes. Again, no gender-associated differences in anti-GFAP antibody immunoreactivity between groups were detected [32]. However, also this conclusion should be drawn with caution as the number of animals per group was limited hampering proper statistical evaluation. In a previous report of our group, TG2 did not colocalise with microglial cells associated with Aβ deposits in APP23 mice [17]. Here, we could also not find evidence for a role of TG2 in microglial presence in microglial cells associated with Aβ deposits in 12-month-old APP23 mice.

Overall, we demonstrated that the absence of TG2 in a human Aβ mouse model significantly reduces the formation and/or deposition of Aβ deposits. Although the set-up of this (cross-sectional) observational study did not allow us to identify causal mechanism(s) linking the lack of TG2 to reduction in Aβ pathology, our data do provide an answer to our research question in suggesting that TG2 may be a feasible target for consideration as part of future therapeutic interventions aiming at reduction of Aβ pathology in AD. As part of this endeavour, among others, future research needs to determine whether the reduction in Aβ pathology is related to TG2's catalytic crosslinking activity of Aβ and/or chaperones involved in the Aβ cascade [9]. Direct protein–protein binding of TG2 with Aβ and TG2-catalysed crosslinking of Aβ have been demonstrated to play role in the TG2-induced Aβ complex and/or aggregate formation by different research groups [12, 22, 31, 49, 50]. Although we here demonstrated that absence of TG2 reduces the formation of Aβ deposits, we cannot disentangle whether this reduction in Aβ deposits is caused by TG2's binding and complex formation with Aβ or TG2's post-translational modification of Aβ through its crosslinking activity. In addition, concentrations of various Aβ oligomers in both APP23 and APP23/TG2−/− mice should be determined to shed more light on the molecular underpinnings of TG2's role in the formation of Aβ deposits. Moreover, the consequences of ablation of TG2 on cognitive performance in APP23/TG2−/− versus on APP23 mice should be investigated. Our data emphasise that in order to gain sufficient statistical power for analysis of such parameters, due to the large variation in Aβ pathology in the APP23 mice model, sufficiently high(er) number of animals need to be included. Also, inclusion of animals of different ages, especially older animals, might provide more insight into TG2's role in the Aβ cascade. Monitoring both the development and levels of Aβ pathology and TG2 levels and activity in vivo could provide crucial information. Interestingly, apart from the widely available Aβ PET ligands to monitor Aβ pathology in vivo, our group recently developed specific PET tracers that could monitor both TG2 levels and activity in vivo [51–53]. Combining data using both PET ligands and the above-described parameters and suggestions will likely unlock the true role of TG2 in the development of Aβ pathology.

ACKNOWLEDGEMENT

We thank Evelien Timmermans-Huisman of the department of Anatomy and Neurosciences for the quantification of the anti-GFAP immunoreactivity. In addition, we thank Allert Jonker of the Department of Anatomy and Neurosciences for assisting in the processing of the mouse material. Part of this work was funded by the Proof-of-Concept Fund of Amsterdam Neuroscience (PoC-2014-ND-06).

CONFLICT OF INTEREST

The authors declare that they have no competing interests.

AUTHOR CONTRIBUTIONS

BD and MMMW designed and analysed the experiments and wrote the manuscript. OC, CAMJ, JGJMB, JJPB and AJ performed the experiments. ML and ABS controlled and conducted the (cross)breeding of all animals used in this study and reviewed the manuscript.

ETHICS STATEMENT

The experimental procedure using the above-mentioned mice were carried out in accordance with the Animal Welfare Body of the VU University and approved by the local Animal Care and Use Committee.

PEER REVIEW

The peer review history for this article is available at https://publons.com/publon/10.1111/nan.12796.

DATA AVAILABILITY STATEMENT

The data that support the findings of this study are available in the Supporting Information of this article.

REFERENCES

1. Selkoe DJ. Amyloid protein and Alzheimer's disease. *Sci Am*. 1991;265(5):68-78. doi:10.1038/scientificamerican1191-68
2. Selkoe DJ. The molecular pathology of Alzheimer's disease. *Neuron*. 1991;6(4):487-498. doi:10.1016/0896-6273(91)90052-2
3. Walsh DM, Lomakin A, Benedek GB, Condron MM, Teplow DB. Amyloid β-protein fibrillogenesis. Detection of a protofibrillar intermediate. *J Biol Chem*. 1997;272(35):22364-22372. doi:10.1074/jbc.272.35.22364
4. Walsh DM, Klyubin I, Fadeeva J V, Rowan MJ, Selkoe DJ. Amyloid-β oligomers: their production, toxicity and therapeutic inhibition. *Biochem Soc Trans*. 2002;30(4):552-557. doi:10.1042/bst0300552
5. Nisbet RM, Götz J. Amyloid-β and tau in Alzheimer's disease: novel pathomechanisms and non-pharmacological treatment strategies. *J Alzheimers Dis*. 2018;64(s1):S517-S527. doi:10.3233/JAD-179907
6. Lorand L, Conrad SM. Transglutaminases. *Mol Cell Biochem*. 1984;58(1-2):9-35. doi:10.1007/BF00240602
7. Lorand L, Graham RM. Transglutaminases: crosslinking enzymes with pleiotropic functions. *Nat Rev Mol Cell Biol*. 2003;4(2):140-156. doi:10.1038/nrm1014
8. Kim SY, Grant P, Lee JH, Pant HC, Steinert PM. Differential expression of multiple transglutaminases in human brain. Increased expression and cross-linking by transglutaminases 1 and 2 in Alzheimer's disease. *J Biol Chem*. 1999;274(43):30715-30721. doi:10.1074/jbc.274.43.30715
9. Wilhelmus MM, de Jager M, Bakker E, Drukarch B. Tissue transglutaminase in Alzheimer's disease: involvement in pathogenesis and its potential as a therapeutic target. *J Alzheimers Dis*. 2014;42(Suppl 3):S289-S303. doi:10.3233/JAD-132492
10. DiRaimondo TR, Klock C, Warburton R, et al. Elevated transglutaminase 2 activity is associated with hypoxia-induced experimental pulmonary hypertension in mice. *ACS Chem Biol*. 2014;9(1):266-275. doi:10.1021/cb4006408
11. Segers-Nolten I, Wilhelmus MM, Veldhuis G, van Rooijen BD, Drukarch B, Subramaniam V Tissue transglutaminase modulates α-synuclein oligomerization. *Protein Sci*. 2008;17(8):1395-1402. doi:10.1110/ps.036103.108
12. Hartley DM, Zhao C, Speier AC, et al. Transglutaminase induces protofibril-like amyloid β-protein assemblies that are protease-resistant and inhibit long-term potentiation. *J Biol Chem*. 2008;283(24):16790-16800. doi:10.1074/jbc.M802215200
13. Wilhelmus MM, van Dam AM, Drukarch B. Tissue transglutaminase: a novel pharmacological target in preventing toxic protein aggregation in neurodegenerative diseases. *Eur J Pharmacol*. 2008;585(2–3):464-472. doi:10.1016/j.ejphar.2008.01.059
14. Grosso H, Mouradian MM. Transglutaminase 2: biology, relevance to neurodegenerative diseases and therapeutic implications. *Pharmacol Ther*. 2012;133(3):392-410. doi:10.1016/j.pharmthera.2011.12.003
15. Johnson GV, Cox TM, Lockhart JP, Zinnerman MD, Miller ML, Powers RE. Transglutaminase activity is increased in Alzheimer's disease brain. *Brain Res*. 1997;751(2):323-329. doi:10.1016/S0006-8993(96)01431-X
16. Wang DS, Dickson DW, Malter JS. Tissue transglutaminase, protein cross-linking and Alzheimer's disease: review and views. *Int J Clin Exp Pathol*. 2008;1(1):5-18.
17. Wilhelmus MMM, de Jager M, Smit AB, van der Loo RJ, Drukarch B. Catalytically active tissue transglutaminase colocalises with Aβ pathology in Alzheimer's disease mouse models. *Sci Rep*. 2016;6(1):20569. doi:10.1038/srep20569
18. Wilhelmus MM, Grunberg SC, Bol JG, et al. Transglutaminases and transglutaminase-catalyzed cross-links colocalize with the pathological lesions in Alzheimer's disease brain. *Brain Pathol*. 2009;19(4):612-622. doi:10.1111/j.1750-3639.2008.00197.x
19. de Jager M, van der Wildt B, Schul E, et al. Tissue transglutaminase colocalizes with extracellular matrix proteins in cerebral amyloid angiopathy. *Neurobiol Aging*. 2013;34(4):1159-1169. doi:10.1016/j.neurobiolaging.2012.10.005
20. Zhang WW, Lempessi H, Olsson Y. Amyloid angiopathy of the human brain: immunohistochemical studies using markers for components of extracellular matrix, smooth muscle actin and endothelial cells. *Acta Neuropathol*. 1998;96(6):558-563. doi:10.1007/s00040010050935
21. Schmid AW, Condemi E, Tuchscherer G, et al. Tissue transglutaminase-mediated glutamine deamidation of β-amyloid peptide increases peptide solubility, whereas enzymatic cross-linking and peptide fragmentation may serve as molecular triggers for rapid peptide aggregation. *J Biol Chem*. 2011;286(14):12172-12188. doi:10.1074/jbc.M110.176149
22. Wilhelmus MMM, Jongenelen CA, Bol JGJM, Drukarch B. Interaction between tissue transglutaminase and amyloid-beta: protein-protein binding versus enzymatic crosslinking. *Anal Biochem*. 2020;592:113578. doi:10.1016/j.ab.2020.113578
23. Wakshlag JJ, Antonyak MA, Boehm JE, Boehm K, Cerione RA. Effects of tissue transglutaminase on β-amyloid1-42-induced apoptosis. *Protein J*. 2006;25(1):83-94. doi:10.1007/s10930-006-0009-1
24. Sturchler-Pierrat C, Abramowski D, Duke M, et al. Two amyloid precursor protein transgenic mouse models with Alzheimer disease-like pathology. *Proc Natl Acad Sci U S A*. 1997;94(24):13287-13292. doi:10.1073/pnas.94.24.13287
25. De Laurenzi V, Melino G. Gene disruption of tissue transglutaminase. *Mol Cell Biol*. 2001;21(1):148-155. doi:10.1128/MCB.21.1.148-155.2001
26. Van Dam D, D'Hooge R, Staufenbiel M, Van Ginneken C, Van Meir F, De Deyn PP. Age-dependent cognitive decline in the APP23 model precedes amyloid deposition. *Eur J Neurosci*. 2003;17(2):388-396. doi:10.1046/j.1460-9568.2003.02444.x
27. Hepp DH, Vergoossen DLE, Huisman E, et al. Distribution and load of amyloid-β pathology in Parkinson disease and dementia with Lewy

bodies. *J Neuropathol Exp Neurol*. 2016;75(10):936-945. doi:10.1093/jnen/nlw070

28. Sturchler-Pierrat C, Staufenbiel M. Pathogenic mechanisms of Alzheimer's disease analyzed in the APP23 transgenic mouse model. *Ann N Y Acad Sci*. 2000;920(1):134-139. doi:10.1111/j.1749-6632.2000.tb06915.x
29. Selkoe DJ. The origins of Alzheimer disease: A is for amyloid. *JAMA*. 2000;283(12):1615-1617. doi:10.1001/jama.283.12.1615
30. Urbanc B, Cruz L, Le R, et al. Neurotoxic effects of thioflavin S-positive amyloid deposits in transgenic mice and Alzheimer's disease. *Proc Natl Acad Sci*. 2002;99(22):13990-13995.
31. Schmid AW, Chiappe D, Pignat V, et al. Dissecting the mechanisms of tissue transglutaminase-induced cross-linking of α-synuclein: implications for the pathogenesis of Parkinson disease. *J Biol Chem*. 2009;284(19):13128-13142. doi:10.1074/jbc.M809067200
32. Eede P, Obst J, Benke E, et al. Interleukin-12/23 deficiency differentially affects pathology in male and female Alzheimer's disease-like mice. *EMBO Rep*. 2020;21(3):e48530. doi:10.15252/embr.201948530
33. Lee J, Kim DE, Griffin P, et al. Inhibition of REV-ERBs stimulates microglial amyloid-beta clearance and reduces amyloid plaque deposition in the 5XFAD mouse model of Alzheimer's disease. *Aging Cell*. 2020;19(2):e13078. doi:10.1111/acel.13078
34. Bailey CD, Johnson G V. Tissue transglutaminase contributes to disease progression in the R6/2 Huntington's disease mouse model via aggregate-independent mechanisms. *J Neurochem*. 2005;92(1):83-92. doi:10.1111/j.1471-4159.2004.02839.x
35. Mastroberardino PG, Iannicola C, Nardacci R, et al. "Tissue" transglutaminase ablation reduces neuronal death and prolongs survival in a mouse model of Huntington's disease. *Cell Death Differ*. 2002;9(9):873-880. doi:10.1038/sj.cdd.4401093
36. Zhang J, Grosso Jasutkar H, Yan R, et al. Transglutaminase 2 depletion attenuates α-synuclein mediated toxicity in mice. *Neuroscience*. 2020;441:58-64. doi:10.1016/j.neuroscience.2020.05.047
37. Leinenga G, Koh WK, Götz J. A comparative study of the effects of Aducanumab and scanning ultrasound on amyloid plaques and behavior in the APP23 mouse model of Alzheimer disease. *Alzheimer's Res Ther*. 2021;13(1):76. doi:10.1186/s13195-021-00809-4
38. Tripathy D, Migazzi A, Costa F, et al. Increased transcription of transglutaminase 1 mediates neuronal death in in vitro models of neuronal stress and Aβ1–42-mediated toxicity. *Neurobiol Dis*. 2020;140:104849. doi:10.1016/j.nbd.2020.104849
39. Wilhelmus MM, Verhaar R, Bol JG, et al. Novel role of transglutaminase 1 in corpora amylacea formation? *Neurobiol Aging*. 2011;32(5):845-856. doi:10.1016/j.neurobiolaging.2009.04.019
40. Wilhelmus MM, Otte-Holler I, Wesseling P, de Waal RM, Boelens WC, Verbeek MM. Specific association of small heat shock proteins with the pathological hallmarks of Alzheimer's disease brains. *Neuropathol Appl Neurobiol*. 2006;32(2):119-130. doi:10.1111/j.1365-2990.2006.00689.x
41. Wilhelmus MM, de Jager M, Rozemuller AJ, et al. Transglutaminase 1 and its regulator tazarotene-induced gene 3 localize to neuronal tau inclusions in tauopathies. *J Pathol*. 2012;226(1):132-142. doi:10.1002/path.2984
42. Janssen L, Keppens C, De Deyn PP, Van Dam D. Late age increase in soluble amyloid-beta levels in the APP23 mouse model despite steady-state levels of amyloid-beta-producing proteins. *Biochim Biophys Acta Mol Basis Dis*. 2016;1862(1):105-112. doi:10.1016/j.bbadis.2015.10.027
43. Battaglia G, Farrace MG, Mastroberardino PG, et al. Transglutaminase 2 ablation leads to defective function of mitochondrial respiratory complex I affecting neuronal vulnerability in experimental models of extrapyramidal disorders. *J Neurochem*. 2007;100(1):36-49. doi:10.1111/j.1471-4159.2006.04140.x
44. de Jager JM, Boot M V, Bol JG, et al. The blood clotting Factor XIIIa forms unique complexes with amyloid-β (Aβ) and colocalizes with deposited Aβ in cerebral amyloid angiopathy. *Neuropathol Appl Neurobiol*. 2016;42(3):255-272. doi:10.1111/nan.12244
45. Citron M, Westaway D, Xia W, et al. Mutant presenilins of Alzheimer's disease increase production of 42-residue amyloid β-protein in both transfected cells and transgenic mice. *Nat Med*. 1997;3(1):67-72. doi:10.1038/nm0197-67
46. van Strien M, de Vries E, Bol JG, et al. Tissue Transglutaminase contributes to the pathogenesis of experimental multiple sclerosis: a role in cell adhesion and migration? *Brain Behav Immun*. 2015;50:141-154. doi:10.1016/j.bbi.2015.06.023
47. van Strien ME, Breve JJ, Fratantoni S, et al. Astrocyte-derived tissue transglutaminase interacts with fibronectin: a role in astrocyte adhesion and migration? *PLoS One*. 2011;6(9):e25037. doi:10.1371/journal.pone.0025037
48. Monteagudo A, Feola J, Natola H, Ji C, Pröschel C, Johnson GVW. Depletion of astrocytic transglutaminase 2 improves injury outcomes. *Mol Cell Neurosci*. 2018;92:128-136. doi:10.1016/j.mcn.2018.06.007
49. Dudek SM, Johnson G V. Transglutaminase facilitates the formation of polymers of the β-amyloid peptide. *Brain Res*. 1994;651(1-2):129-133. doi:10.1016/0006-8993(94)90688-2
50. Ikura K, Takahata K, Sasaki R. Cross-linking of a synthetic partial-length (1-28) peptide of the Alzheimer β/A4 amyloid protein by transglutaminase. *FEBS Lett*. 1993;326(1-3):109-111. doi:10.1016/0014-5793(93)81772-R
51. van der Wildt B, Wilhelmus MMM, Bijkerk J, et al. Development of carbon-11 labeled acryl amides for selective PET imaging of active tissue transglutaminase. *Nucl Med Biol*. 2016;43(4):232-242. doi:10.1016/j.nucmedbio.2016.01.003
52. van der Wildt B, Wilhelmus MMM, Kooijman EJM, et al. Development of fluorine-18 labeled peptidic PET tracers for imaging active tissue transglutaminase. *Nucl Med Biol*. 2017;44:90-104. doi:10.1016/j.nucmedbio.2016.10.002
53. van der Wildt B, Wilhelmus MMM, Beaino W, et al. In vivo evaluation of two tissue transglutaminase PET tracers in an orthotopic tumour xeno3graft model. *EJNMMI Res*. 2018;8(1):39. doi:10.1186/s13550-018-0388-2

SUPPORTING INFORMATION

Additional supporting information may be found in the online version of the article at the publisher's website.

How to cite this article: Wilhelmus MMM, Chouchane O, Loos M, et al. Absence of tissue transglutaminase reduces amyloid-beta pathology in APP23 mice. *Neuropathol Appl Neurobiol*. 2022;48(4):e12796. doi:10.1111/nan.12796